buildings

MDPI

Article

Extrusion and Subsequent Transformation of Textile-Reinforced Mortar Components—Requirements on the Textile, Mortar and Process Parameters with a Laboratory Mortar Extruder (LabMorTex)

Matthias Kalthoff *, Michael Raupach and Thomas Matschei

Institute of Building Materials Research (IBAC), RWTH Aachen University, Schinkelstraße 3, 52062 Aachen, Germany; raupach@ibac.rwth-aachen.de (M.R.); matschei@ibac.rwth-aachen.de (T.M.)
* Correspondence: matthias.kalthoff@rwth-aachen.de; Tel.: +49-241-80-95-143

Abstract: To produce defect-free extruded and shaped components, the forming behaviour of extruded fibre-reinforced mortar mixtures, impregnated textiles and extruded textile-reinforced mortar (TRM) was investigated. The TRM test specimens were formed longitudinally and transversely using specially developed forming setups. Regardless of the selected fibre content ranging between 0 and 0.5 Vol.-%, defect-free longitudinal forming of the mortar is possible up to a bending radius of 5 cm and transversely up to a bending radius of approx. 6 cm. For the extruded TRM specimens, longitudinal bending radii of up to 10 cm were achieved. The results represent the basis for the construction of new formwork-free extruded and subsequently shaped textile-reinforced concrete components.

Keywords: extrusion; pultrusion; textile-reinforced concrete (TRC); carbon concrete

Citation: Kalthoff, M.; Raupach, M.; Matschei, T. Extrusion and Subsequent Transformation of Textile-Reinforced Mortar Components—Requirements on the Textile, Mortar and Process Parameters with a Laboratory Mortar Extruder (LabMorTex). *Buildings* **2022**, *12*, 726. https://doi.org/10.3390/buildings12060726

Academic Editor: Jorge de Brito

Received: 11 May 2022
Accepted: 25 May 2022
Published: 26 May 2022

1. Introduction

Currently, intensive research in the field of concrete construction is underway to develop production methods that minimise the use of resources while keeping the structural carbon footprint as small as possible [1]. Two key strategies are to increase the use of materials that have a low carbon footprint and to develop new principles for designing material-minimised components [2–4].

To design material-minimised components, the structures must be designed following force flow principles and the material must meet the required strength criteria. This construction principle is not new and was previously implemented by the Romans, e.g., during the construction of archways. The aim of those arches or chain shapes is that the structure is formed free of any detrimental momentums [5]. However, the main challenge is to determine that acting forces that must be considered in the model, since it is not possible to optimise a structure for every load case. Consequently, the critical load case combination needs to be found and considered during the form finding process [5,6]. If the structure has a high dead weight, the archway should have the shape of the cosine hyperbolicus, and if the traffic loads are high, it should have the shape of a parabola [7,8]. Examples of this type of construction are presented in Figure 1a,b.

(a) (b)

Figure 1. (**a**) The Gateway Arch in St. Louis, USA [9]; (**b**) Gaudí's hanging model [10].

The use of textile-reinforced concrete (TRC) is particularly suitable to produce these components. Instead of steel, fibres made of glass, basalt or carbon are used as reinforcement, which are processed from endless rovings into textile structures, usually with a polymer impregnation. In recent years, flexible impregnations based on styrene-butadiene rubber (SBR), Polyacrylat (PA) and stiff impregnations with epoxy resin have prevailed. To date, stiff impregnated textiles have achieved higher tensile strengths, since they ensure an even load transfer between the fibres in the roving [11,12]. Depending on the impregnation material and quality, carbon textiles have a tensile strength 5 to 8 times higher than that of steel. In addition, having a density of approx. 1700 kg/m^3, they are more than 4 times lighter than conventional concrete steel rebars [13–15]. Furthermore, in the absence of any corrosion problems, the minimum concrete cover can be significantly reduced during the production of carbon concrete components, i.e., a concrete cover of at least 5 mm to ensure significant bonding, and requirements relating to the concrete maximum aggregate size must be complied with.

For the production of TRC structure lamination, casting [16] or spraying processes are mainly used [17]. An innovative method is the production of TRC structures by means of extrusion [18]. Currently, unreinforced or microfibre-reinforced concrete components are already extruded at an industrial scale [19,20]. High demands are placed on the rheological properties of the fresh concrete. The concrete must be conveyable within the extruder, while also having the desired shape, and thus a sufficient green strength after leaving the mouthpiece [19].

In [20], various fibres were investigated in combination with the extrusion process. The results show that both PVA and basalt fibres are generally suitable for concrete extrusion. However, the use of aramid fibres resulted in deterioration of the concrete consistency due to their high water absorption; thus, a defect-free extrusion was not possible. Carbon fibres also proved unsuitable for the extrusion process, as they broke in the mixer due to their sensitivity to transversal pressure.

In [19], multiple test setups were investigated to determine the suitability of fresh concrete for the extrusion process even before the actual extrusion process. In [21], based on the investigations from [22,23], a novel method was developed that allows the integration of stiff impregnated textiles in the extrusion process and thus high-performance materials can be produced with high accuracy and tensile strength up to 2200 MPa. The extrusion process enables much simpler reinforcement integration compared to currently pursued 3D concrete printing approaches based on layer-by-layer extrusion. Currently, however, there is a lack of a process in which textile concrete components are specifically formed after the extrusion process.

Various other manufacturing methods exist to produce concrete components that follow form-follows-force pathways. In [24,25], extensive investigations were published concerning folding of textile concrete structures. In general, a distinction is made between two folding methods: the fold-in-fresh principle, in which the fresh concrete is formed by moving the formwork, and the fold-and-grout principle, where the concrete is first curved and then folded over joints. Different modules are produced, folded and then assembled by means of bolts or filled joints. The chosen folding forms are mainly origami or yoshimur [26].

In [27], a biaxial textile with locally adjusted bending stiffness was used for the folding process. In the area of the folding joints, the textile was made flexible to allow folding at these points. In the rest of the cross-section, the textile was stiff. In [28], a thin-vaulted concrete floor was developed according to a finding and fabrication process with specific geometries that carried 2.5 times the factored design load in a more critical asymmetric loading scenario.

In this study, the forming behaviour of extruded fibre-reinforced mortar and textile-reinforced mortar components was investigated in order to create the basis for producing material-minimised and load-path-compatible components with the aid of extrusion. The technical limits of the forming behaviour immediately after extrusion and the influence of the microfibres, in addition to the different textile reinforcements, are not yet known.

2. Materials

Currently, there is a lack of valid test results to produce formed textile-reinforced mortar (TRM) components with the aid of a laboratory mortar extruder (LabMorTex). Therefore, extensive investigations were carried out on TRM components as part of this work. First, five different mortar mixtures were developed that differed significantly in their microfibre content and fibre material. In addition, basalt and PVA microfibres were used for comparison. The reference, mixture 1, was produced without microfibres. An overview of the mixtures is given in Table 1. The compressive strength was determined on 40 mm^3 × 40 mm^3 × 160 mm^3 mortar prisms following DIN EN 196-1 [29] at the age of 28 days. The samples were stored under water until the mortar was 7 days old and then at 20 °C and 65% rel. humidity. The aim of the investigation was to determine the minimum fibre content required to ensure an extrudable mortar mixture, without defects, that also remained flexible enough to allow subsequent fresh-in-fresh folding processes.

Table 1. Mix design of the investigated mortars.

Components	Unit	1	2	3	4	5
CEM I 42,5 R	kg/m^3			700		
Silica powder				70		
Fly ash				210		
Water				278		
Sand 0.1–0.5 mm		678	676	670	676	670
Quartz powder 0–0.250 mm		283	279	278	279	278
Methyl cellulose				7.0		
PVA microfibres	Vol.-%	-	-	-	0.25	0.50
Basalt microfibres		-	0.25	0.50	-	-
Compressive strength 28d	MPa	62	64	63	62	65

In addition, investigations with textile reinforcements were carried out on mortar mix 5. The carbon textile SITgrid044 VL and the glass textile AR-240 were used as reinforcement. Both textiles have a polymer impregnation. The exact composition is subject to the respective company secrets. The two textiles are shown in Figure 2a,b.

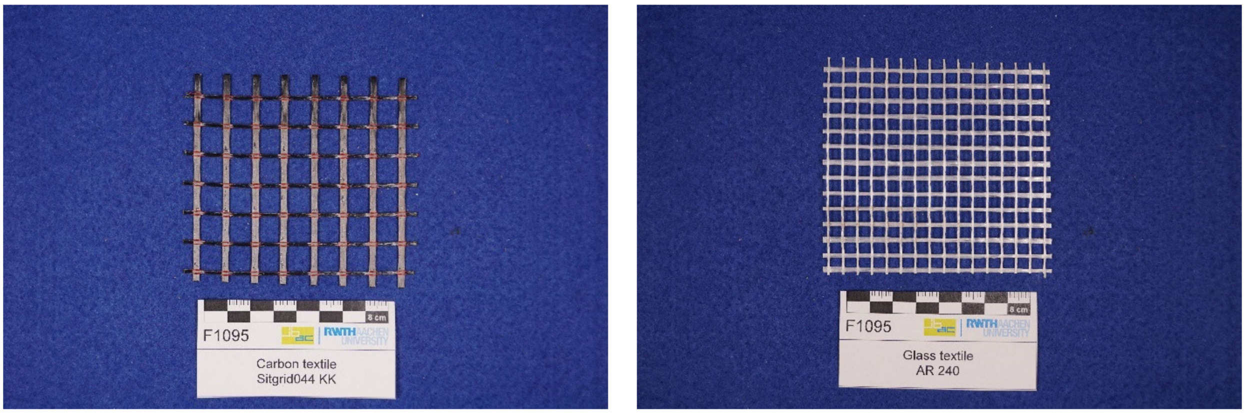

(**a**) (**b**)

Figure 2. (**a**) Carbon textile SITgrid044 VL; (**b**) glass textile AR 240.

The properties of the textiles used are shown in Table 2.

Table 2. Material properties of SITgrid044 VL according to [21].

Textile Reinforcement	Fibre Material	Tensile Strength (1)	Modulus of Elasticity (1,2)	Fineness (1)	Mesh Size (1)	Cross Section per m (1)	Basis Weight
-		MPa	GPa	Tex	mm	mm^2	g/m^2
SITgrid044 VL	Carbon	1840	150	1010	12	35.3	186
AR 240	Glass	1064	49	770	5	48.3	263

(1) Warp and weft direction; (2) In relation to the total cross-section.

3. Experimental Methods and Shaping Process

3.1. Mortar Production

Analogous to the studies in [21], an Eirich R05T intensive mixer with a maximum capacity of 40 litres was used to produce the mortars for the extrusion process. The motor data, the temperature in the mixer and the resistance torque were recorded during all mixing processes. For each batch, 18 litres of fresh mortar were produced. First, the dry components were homogenised at 500 revolutions per minute for a duration of a minute. Then, the water was added within 15 s at 66 revolutions per minute. The mortar was then mixed for a further 130 s at 800 rpm. Finally, the mixing speed was reduced at intervals of 100 revolutions per minute every 15 s to investigate the rheological behaviour of the mixtures at different step profiles. During the mixing process, the mixing data were also recorded.

3.2. Mortar Extrusion Process

A Händle laboratory extruder was used for the extrusion of the plain-, fibre- and textile-reinforced mortars. The extrusion process of the laboratory mortar textile extruder (LabMorTex) was previously presented in detail in [21]. Therefore, the procedure is only briefly described here. The extruder consists of a pre-press and an auger. Various mouthpieces with different geometries can be attached to the end of the auger. In the transition area between the pre-press and the auger, it is also possible to generate a vacuum, which de-airs, compacts and compresses the extrudate. Figure 3a shows a photo of the LabMorTex and Figure 3b shows a schematic drawing of the extruder. After the mortar leaves the mouthpiece, it is transported on a conveyor belt.

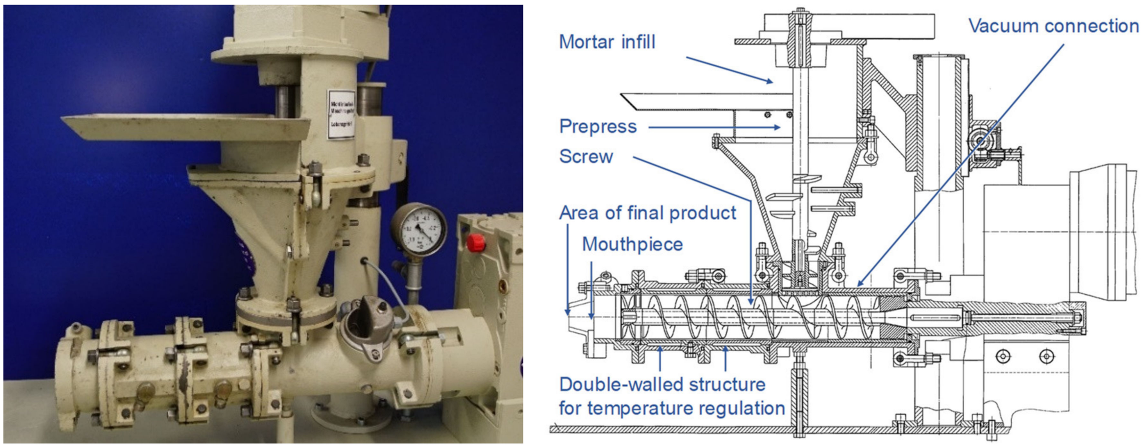

(**a**) (**b**)

Figure 3. (**a**) Laboratory mortar extruder (LabMorTex) [21]; (**b**) schematic drawing of the LabMorTex [21].

Immediately at the end of the auger, the pressure in bar and the temperature in °C are measured during extrusion. In addition, the speed in rpm, the motor current in amperes of the auger and pre-press, and the negative pressure generated by the vacuum pump are monitored. By means of a measuring impeller, it is also possible to assess the conveyor belt speed.

3.3. Determination of the Bending Stiffness of the Textiles

To determine the bending stiffness of the used textiles, a modified test setup of the cantilever test described in [30] was used. With this method, the resistance of textile fabrics is determined using the resulting bending stress because of the fabrics' own weight. The test was initially developed to examine unimpregnated textiles. To test the impregnated textiles used in this work, the cantilever test setup had to be modified further. The textiles examined had a length of 1000 mm and a width of 55 mm. This also corresponds to the dimensions of the textiles for the extrusion process.

The flexural rigidity of the textiles can be determined using the cantilever method with the help of the deflection of the textiles in dependence on the overhang length. The deflection $w_{50.1}$ was determined on the edge of the side parts with a horizontal free test length of 50.1 cm on very stiff textiles that protruded beyond the side parts of the test setup. If the textile crossed the side parts of the flexural rigidity tester, the deflection $w_{55.0}$ was measured at an overhang length of 55.0 cm. Based on the results, the bending radius was determined. A schematic illustration of the experimental setup is shown in Figure 4.

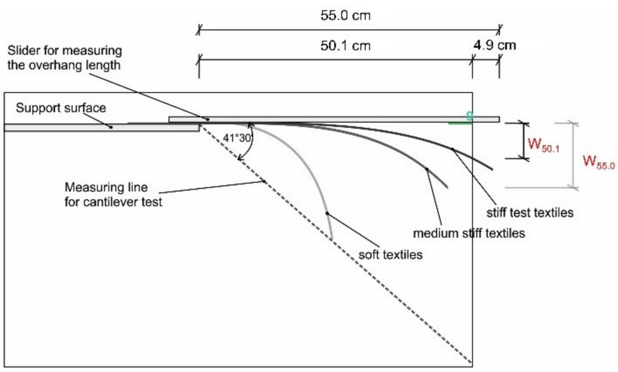

Figure 4. Schematic illustration of the determination of the bending stiffness of stiff, medium stiff and soft textiles.

The flexural rigidity was calculated as follows:

$$B = F_1 * \left(\frac{l_{\text{Ü}}}{2}\right)^3 * 10^{-2} \tag{1}$$

with:

B Flexural stiffness in N cm^2
F_1 Length Weight force in N/m
$l_{\text{Ü}}$ Overhang length of the sample in cm

F_1 is the length-related weight of the specimen and is calculated from the quotient of the mass of the specimen and its length, multiplied by the specific gravity of 9.81 m/s^2. The previously determined textile weight per unit area was used to calculate the linear weight force of the strip samples. The area-related mass was multiplied by the width of the textile strips, resulting in the length-related mass. The linear weight force was calculated according to Equation (2):

$$F_1 = g * (M * b) * 10^{-3} \tag{2}$$

where:

F_1 Length weight force in N/m
g acceleration of gravity in m/s^2
M Weight of the textile in g/m^2
b Width of the specimen in m

By means of the vertical deflection, the bending stiffness was calculated by considering a cantilever arm and assuming a point load F_1 at the end of the cantilever arm, as described in Equation (3):

$$EI = \frac{F_1 * {l_{\text{ü}}}^4}{3 * w} \tag{3}$$

where:

EI Bending stiffness in N cm^2
F_1 Length weight force in N/m
$l_{\text{ü}}$ Overhang length of the sample in cm
w Deflection of the specimen in cm

3.4. Shaping Process

One objective of this study was to determine the minimal bending radius for the extruded mortar specimens. In order to produce thin and, at the same time, high-performance components from textile-reinforced mortar, test specimens with a length of approx. 1200 mm and a cross-sectional area of 60 × 10 mm were selected. The cross-sectional geometry is also dependent on the LabMorTex used, as only small-format specimens can be produced due to the small size. The determined bending radii serve as a basis for the subsequent design of formed components, preferably in accordance with the load path. Therefore, the extruded mortar was shaped in longitudinal and transverse directions. Therefore, two shaping procedures were developed.

For the assessment of the minimal bending radius in the transverse direction, pipes of different diameters were used. An overview of the pipes used can be found in Figure 5. The advantage of using pipes is that their bending radius is defined and that they have a smooth surface. Thus, the extruded mortar could be placed parallel to the axis of symmetry of the pipe. The fresh mortar was shaped according to the bending radius of the pipe solely by gravity. Pipes of the following diameter were used: Diameter Nominal (DN) 160, DN 110, DN 75, and DN 50.

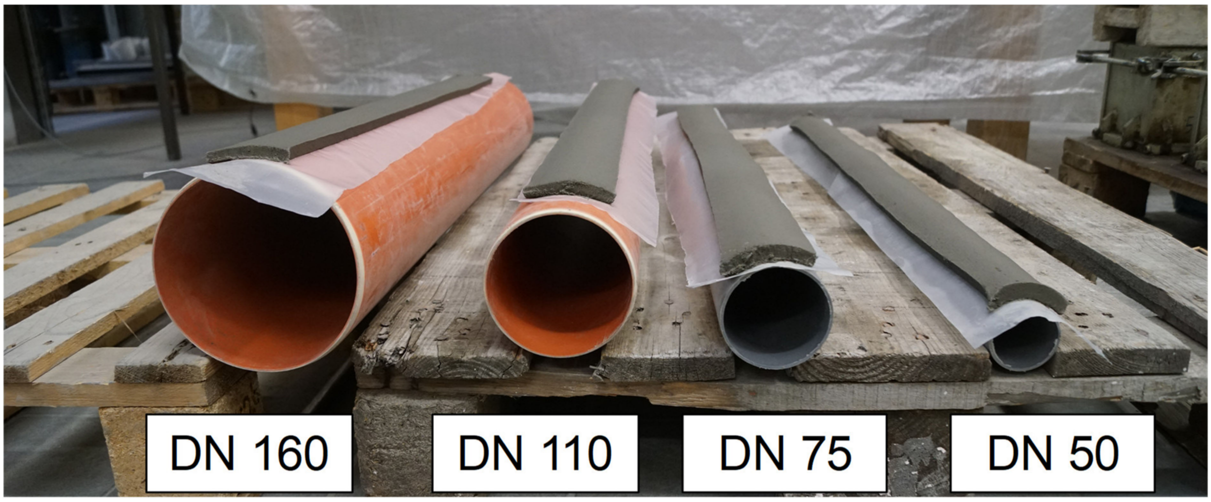

Figure 5. Pipes for shaping extruded components in the transverse direction from DN 160 to DN 50.

It was observed that the fresh mortar mixture of the applied mix designs was too stiff to be formed transversally along the pipes' cross-section only by gravity. Therefore, especially for the small pipes, the mortar was pressed softly with rolls against the pipes to achieve the desired radius of curvature.

For the evaluation of the minimal bending radius in the longitudinal direction, another test setup was developed that allowed a flexible adjustment of the bending radius. A photo of the experimental setup is shown in Figure 6a and a technical drawing in Figure 6b. This test setup was designed to allow the mortar to hang freely between two attachment points, thus corresponding to the catenary arch described in the introduction. Depending on the desired bending radius, the distance between the two fixed points can be changed by altering the support distances. The procedure is also shown in Figure 6a. The designed test setup consists of five individually adjustable tracks. Each track has two clamping jaws that serve as fixing points for the hanged mortar specimen.

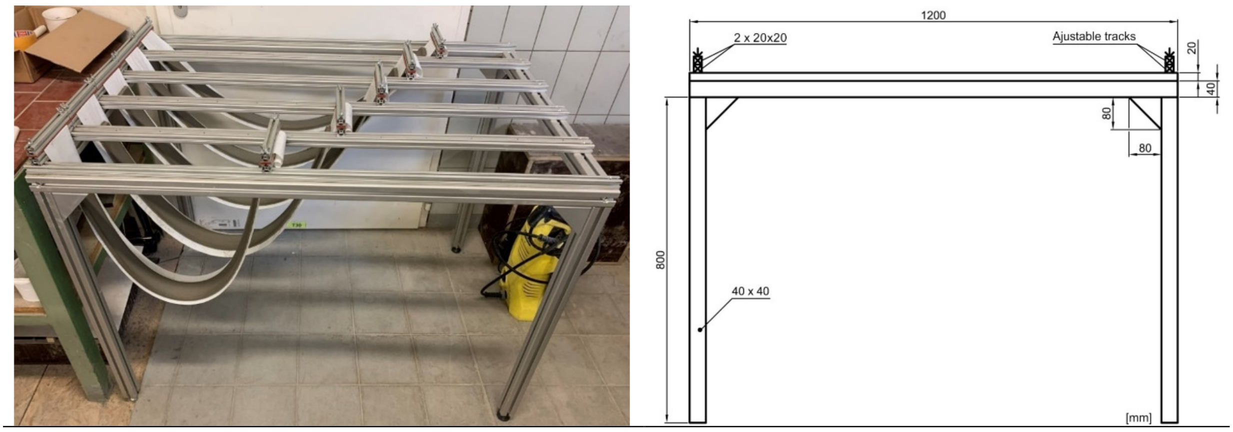

(**a**) (**b**)

Figure 6. (**a**) Example of the formed specimens in the longitudinal direction; (**b**) drawing of the experimental setup for reshaping in the longitudinal direction.

The reshaping in the longitudinal direction was undertaken for all mixtures 1–5. In addition, the shaping tests were performed with the extruded mortar specimens of series 5 with both the glass and carbon textiles. The specimens were analysed at the mortar age of one day.

4. Results

4.1. Bending Stiffness of the Textiles

Figure 7 shows the bending stiffness and bending radius of the textile strip specimens with the knitted rovings oriented upwards (blue) and downwards (red) in N cm^2 and cm, respectively. The investigated glass textile has a significantly lower bending stiffness than the carbon textile. With an average bending stiffness of 21 N cm^2, the glass textile exhibits low resistance to deformation. The carbon textile, on the other hand, has a bending stiffness of around 420 N cm^2. The bending stiffness of the carbon textile is thus 20 times higher than that of the glass textile used. When determining the bending radius, smaller differences were found, although the glass textile has a bending radius of 25 cm, which is about 4.3 times smaller than that of the carbon textile used, due to its own weight. The storage direction of the knitting yarns does not seem to have a major influence on the respective deformation behaviour for either textile. The bending stiffness of the textiles thus depends on the fineness of its roving, but mainly on the impregnation applied and its stiffness. However, this statement still needs to be confirmed by further investigations.

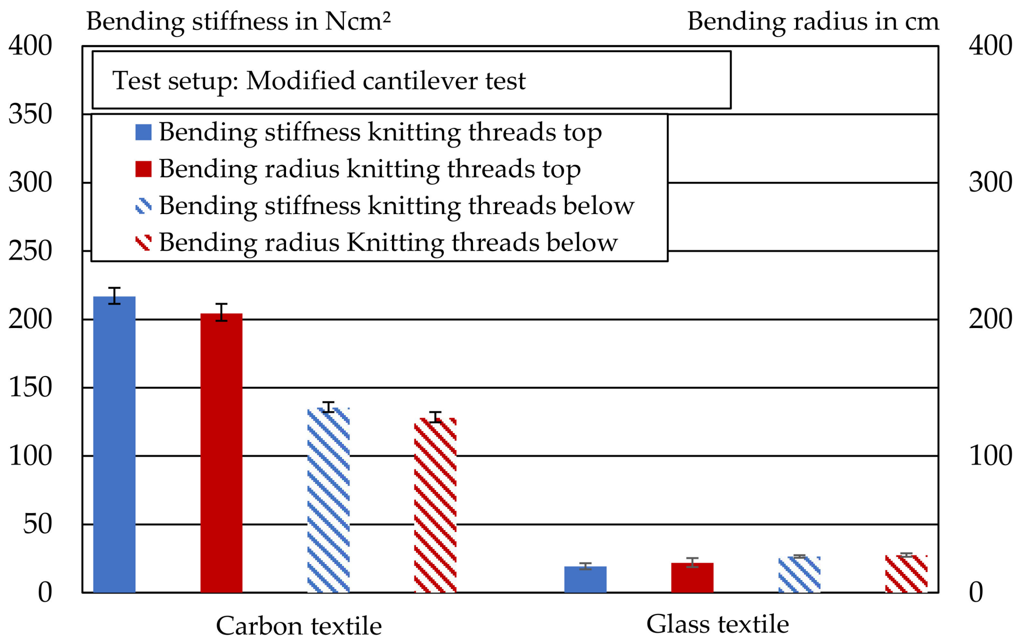

Figure 7. Bending stiffness and bending radius of the carbon and glass fibre textiles depending on the orientation of the knitting thread.

4.2. Shaping Behavior of the Mortar

Figure 8a shows the calculated target bending radius dependent of the chosen distances and the actually measured radius for the transverse forming for all five mixtures. The bending radius was adjustable between 3.8 cm and approx. 8.0 cm for all the mixtures investigated. Figure 8b shows the maximum crack width above the measured bending radius. It can be observed that, below a bending radius of approx. 5 cm, cracks up to a width of 0.3 mm appeared on the surface, regardless of the fibre type and content.

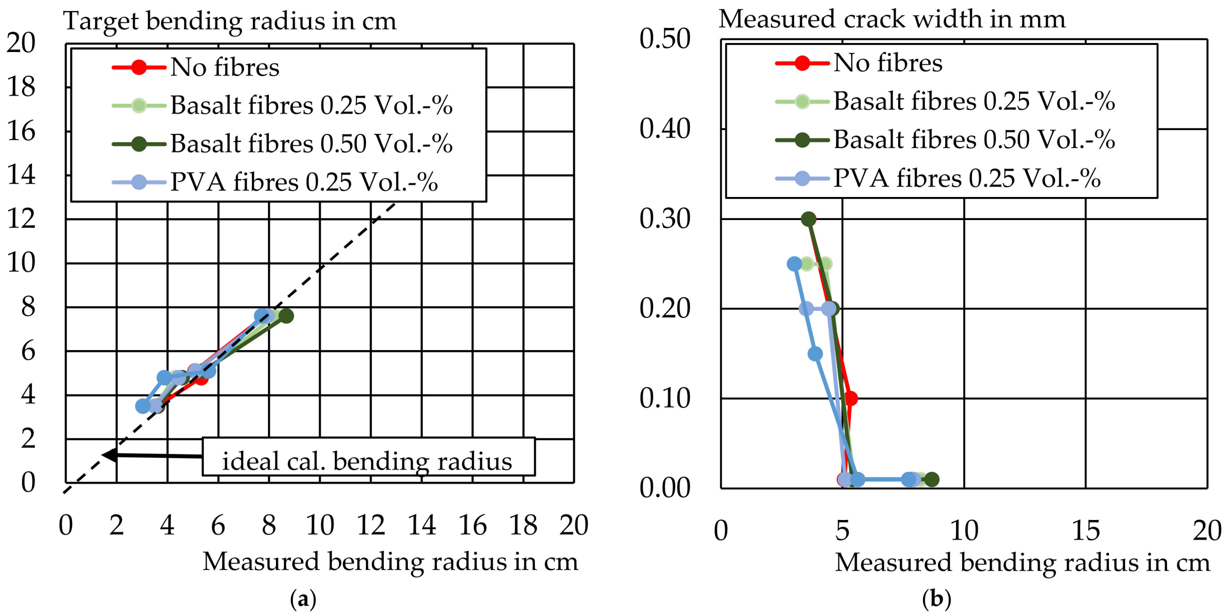

Figure 8. (**a**) Target and the measured bending radius for the transverse forming of the extruded mortar specimens; (**b**) crack width vs. measured bending radius for the transverse deformation of the extruded mortar specimens.

Accordingly, the technical limit for crack-free transverse shaping of extruded plain mortar and microfibre-reinforced mortars with a cross-sectional dimension of 10 × 60 mm^2 lies at around 6 cm. An example of a cracked specimen in the transverse direction is shown in Figure 9a,b. Contrary to expectations, neither fibre type or fibre content significantly affected the shaping behaviour and crack initiation of the extruded mortar specimens.

Figure 9. (**a**) Bottom of transversally formed mortar specimen of mixture 1 with visible cracks of approx. 0.4 mm, bending radius approx. 3.8 cm; (**b**) side view of transversally formed mortar specimen of mixture 1, radius approx. 3.8 cm.

The results of the shaped extruded fibre-reinforced specimens in the longitudinal direction are shown in Figure 10a. Above a calculated target radius of 10 cm, the specimens do not achieve the desired curvature, although bending radii of up to 5 cm are possible regardless of fibre content and fibre type. A curvature based on the catenary arch can thus be set relatively easily with the new experimental setup using extruded specimens having a cross-sectional area of 10 × 60 mm^2.

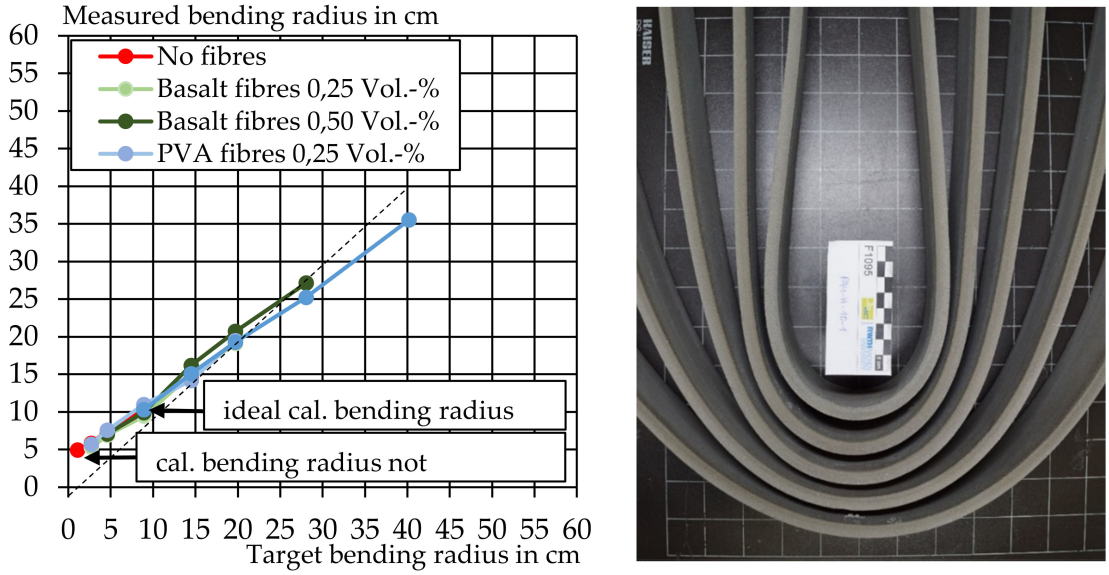

(**a**) (**b**)

Figure 10. (**a**) Calculated target and the measured bending radius for the longitudinal forming of the extruded mortar specimens; (**b**) longitudinally formed mortar specimen without visible cracks (no fibres and no textile reinforcement).

In contrast to the transversely formed specimens, no cracks were detected on the surface of any longitudinally formed mortar specimens, although the bending radius of only 5 cm is very small. Analogous to transversal forming, the restriction for crack-free deformation in the longitudinal direction does not appear to be determined by the mortar or fibres for the cross-sectional dimension studied. An example of a formed specimen in the longitudinal direction is shown in Figure 10b.

4.3. Bending Behaviour of Extruded Textile-Reinforced Mortar

Similar to the experiments with the unreinforced and microfibre-reinforced specimens, the longitudinal and transverse bending behaviour of extruded TRM was investigated. It was found that transverse bending could not be performed in a permanent controllable manner. As can be seen in Figure 11a, the textiles inhibit transverse bending since they kink due to their stiffness. A permanent intentional deformation only took place in the edges, where there was no textile reinforcement. A targeted and controlled transverse forming for the cross-sectional area of $60 \times 10\ \text{mm}^2$ was, therefore, not possible. The bending attempt even led to a local delamination of the textile from the mortar.

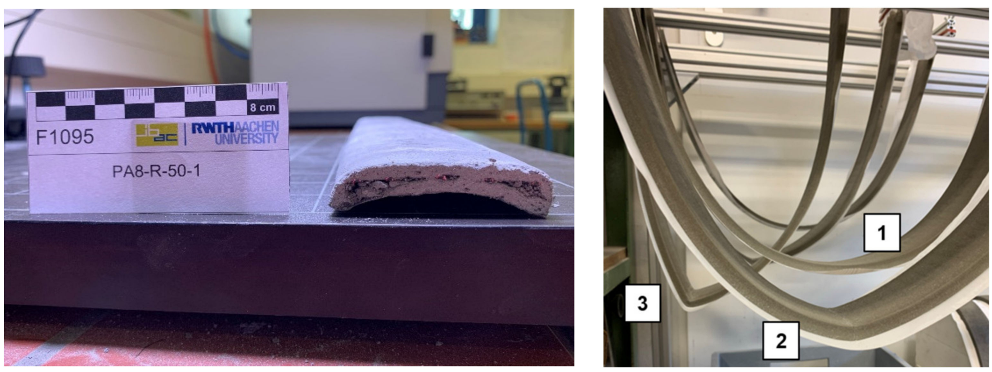

(**a**) (**b**)

Figure 11. (**a**) Extruded and subsequently transversely formed carbon TRM specimen; (**b**) extruded and subsequently longitudinally formed carbon TRM specimens.

In contrast, bending of the TRM specimens in the longitudinal direction was successfully implemented with the specially developed experimental setup. However, in contrast to the non-reinforced specimens, errors occurred during forming. Examples of these forming defects are shown in Figure 11b.

During bending, only some specimen could be successfully reshaped without defects (cf. Figure 11b specimen 1). However, in specimens 2 and 3, buckling appeared in the lower part of the specimen. This type of failure suggests that the textile in the mortar buckled because of the forming process, causing the deformation failure. The small cross-sectional dimension of 60 × 10 mm can further intensify the effect, as the very thin components are prone to buckling. An overview of the achieved bending radius of TRM specimens is shown in Figure 12. It is noteworthy that the bending radii for successful forming of TRM specimens with either glass or carbon textiles show similar behaviour. Based on the results of the forming properties of the textile reinforcements (bending stiffness and bending radius) in Section 4.1 (cf. Figure 7), it was expected that the TRM specimens with carbon reinforcement are only suitable for comparatively large bending radii from 25 cm for the glass textile and 130 cm for the carbon textile.

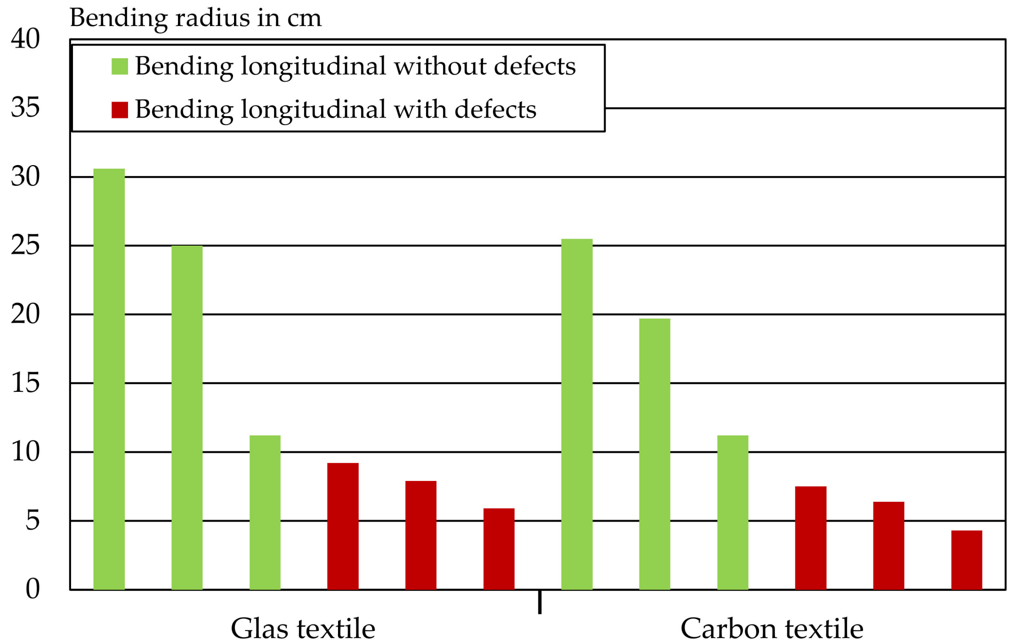

Figure 12. Bending radius for extruded and subsequently longitudinally shaped glass and carbon TRM specimens.

For the carbon TRM, bending radii of approx. 10 cm were achieved without cracks forming or defects occurring. Compared to fibre-reinforced mortar, bending radii that are only twice as large as those of the fibre-reinforced mortar can be achieved with carbon TRM specimens during longitudinal forming. However, the bending radii of the TRM specimens were 13 times smaller than the bending radii determined for the textile reinforcement with the modified cantilever test. Thus, the cantilever test does not seem to be suitable for describing the forming behaviour of the textiles in the extruded TRM specimens with a cross-section of 60 × 10 mm^2. The developed experimental setup (cf. Section 3.3) for longitudinal forming of the extruded specimens, by comparison, is much more suitable for this type of investigation.

The results show that the extrusion process can be used to produce unreinforced, fibre-reinforced and TRM specimens, and subsequently shape them. It was shown that a comparatively small bending radius can be realised, and thus the basis for the design of shaped TRM is possible.

Unlike the folding process in [24,26,31] or [25], complex formwork is no longer necessary for both the production of the TRM and the forming. Considering the results from [21], it can be concluded that extrusion is suitable for the production of thin high-performance TRM and subsequent forming.

5. Conclusions

The production of subsequently formed thin fibre-reinforced mortar and TRM components poses a particular challenge of extrusion technology. In this work, the forming behaviour of extruded specimens with a LabMorTex was investigated and technical limits for maximum bending radii were identified. The results indicate that pressure elements with a high geometrical variety can be designed and built with high quality. The main results achieved in this experimental study are:

- Regardless of the selected fibre content, neither the PVA nor the basalt microfibres used had a significant influence on the bending behaviour of the freshly extruded specimens produced with the LabMorTex.
- The modified cantilever test is a suitable method to characterise the bending behaviour of impregnated textiles otherwise it is not able to describe the behaviour of textiles inside TRM components in a accurate way.
- With the newly developed experimental setup for shaping in the longitudinal direction, a longitudinal bending radius of only 5 cm can be achieved.
- Fibre-reinforced specimens with bending radii of up to approx. 5 cm were produced without surface defects or cracks. For the glass textile and carbon textile-reinforced specimens, longitudinal bending radii of up to approx. 10 cm were determined.
- During transverse forming, bending radii of approx. 6 cm were determined without defects for fibre-reinforced specimens, regardless of the fibre type and content. In the case of TRM specimens, it was not possible to produce flawless specimens while transversely forming.

Author Contributions: Conceptualization, methodology, software, validation, formal analysis, investigation, resources, data curation, writing—original draft preparation, M.K.; writing—review and editing, M.K., M.R. and T.M.; visualization, supervision, project administration, M.K.; funding acquisition, M.R. and T.M. All authors have read and agreed to the published version of the manuscript.

Funding: This research was funded by Deutsche Forschungsgemeinschaft (DFG, German Research Foundation)–SFB/TRR 280. Projekt-ID: 417002380.

Institutional Review Board Statement: Not applicable.

Informed Consent Statement: Not applicable.

Acknowledgments: The authors would like to thank the DFG for supporting the research project.

Conflicts of Interest: The authors declare no conflict of interest.

References

1. Adesina, A. Recent advances in the concrete industry to reduce its carbon dioxide emissions. *Environ. Chall.* **2020**, *1*, 100004. [CrossRef]
2. Lu, W.; Lee, W.M.; Xue, F.; Xu, J. Revisiting the effects of prefabrication on construction waste minimization: A quantitative study using bigger data. *Resour. Conserv. Recycl.* **2021**, *170*, 105579. [CrossRef]
3. Beckmann, B.; Bielak, J.; Bosbach, S.; Scheerer, S.; Schmidt, C.; Hegger, J.; Curbach, M. Collaborative research on carbon reinforced concrete structures in the CRC/TRR 280 project. *Civ. Eng. Des.* **2021**, *3*, 99–109. [CrossRef]
4. Janani, R.; Lalithambigai, N. A critical literature review on minimization of material wastes in construction projects. *Mater. Today Proc.* **2021**, *37*, 3061–3065. [CrossRef]
5. Lewis, W.J. Tension cables in suspension bridges. A case of form-finding. In *Tension Structures: Form and Behaviour*, 2nd ed.; Lewis, W.J., Ed.; ICE Publishing: London, UK, 2017; pp. 101–133; ISBN 978-0-7277-6173-6.
6. Lewis, W. Form-Finding Approach to Modelling Minimal Structural Forms, With Analogy to Nature. In Proceedings of the ISSA 2016: Innovative Structural Systems in Architecture, Wroclaw, Poland, 3–5 November 2016; pp. 39–42.
7. Lewis, W.J. Mathematical model of a moment-less arch. *Proc. R. Soc. A* **2016**, *472*, 1–14. [CrossRef] [PubMed]

8. Heyman, J. Hooke's cubico–parabolical conoid. *Notes Rec. R. Soc. Lond.* **1998**, *52*, 39–50. [CrossRef]
9. Buphoff. Gateway Arch, 2007: Permission of Use: CC BY-SA 3.0. Available online: https://de.wikipedia.org/wiki/Gateway_Arch_National_Park#/media/Datei:STL_Skyline_2007_crop_(Gateway_Arch).jpg (accessed on 16 April 2021).
10. Maher, A.; Burry, M. The Parametric Bridge: Connecting Digital Design Techniques in Architecture and Engineering. In Proceedings of the 2003 Annual Conference of the Association for Computer Aided Design in Architecture, Indianapolis, IN, USA, 23–26 October 2003; pp. 39–47.
11. Morales Cruz, C. Crack-Distributing Carbon Textile Reinforced Concrete Protection Layers. Ph.D. Thesis, RWTH Aachen University, Aachen, Germany, 2020. [CrossRef]
12. Rempel, S. Reliability of the Structural Design for Concrete Elements with Textile Reinforcement and Bending Load. Ph.D. Thesis, RWTH Aachen University, Aachen, Germany, 2018. [CrossRef]
13. Bielak, J. Shear in Slabs with Non-Metallic Reinforcement. Ph.D. Thesis, RWTH Aachen University, Aachen, Germany, 2021. [CrossRef]
14. Halvaei, M.; Jamshidi, M.; Latifi, M.; Ejtemaei, M. Experimental investigation and modelling of flexural properties of carbon textile reinforced concrete. *Constr. Build. Mater.* **2020**, *262*, 120877. [CrossRef]
15. May, S.; Steinbock, O.; Michler, H.; Curbach, M. Precast Slab Structures Made of Carbon Reinforced Concrete. *Structures* **2019**, *18*, 20–27. [CrossRef]
16. Schladitz, F.; Lorenz, E.; Jesse, F.; Curbach, M. Verstärkung einer denkmalgeschützten Tonnenschale mit Textilbeton. *BUST* **2009**, *104*, 432–437. [CrossRef]
17. Brameshuber, W. Manufacturing methods for textile-reinforced concrete. In *Textile Fibre Composites in Civil Engineering*; Elsevier: Amsterdam, The Netherlands, 2016; pp. 45–59. ISBN 9781782424468.
18. Zhou, X.; Li, Z. Manufacturing cement-based materials and building products via extrusion: From laboratory to factory. *Proc. Inst. Civ. Eng.-Civ. Eng.* **2015**, *168*, 11–16. [CrossRef]
19. Alfani, R.; Guerrini, G.L. Rheological test methods for the characterization of extrudable cement-based materials—A review. *Mater. Struct.* **2005**, *38*, 239–247. [CrossRef]
20. Perrot, A.; Rangeard, D.; Nerella, V.N.; Mechtcherine, V. Extrusion of cement-based materials—An overview. *RILEM Tech. Lett.* **2018**, *3*, 91–97. [CrossRef]
21. Kalthoff, M.; Raupach, M.; Matschei, T. Investigation into the Integration of Impregnated Glass and Carbon Textiles in a Laboratory Mortar Extruder (LabMorTex). *Materials* **2021**, *14*, 7406. [CrossRef] [PubMed]
22. Janissen, L.; Raupach, M.; Hartung-Mott, R. Extrusion faserverstärkter Textilbetone. *Bautechnik* **2019**, *96*, 723–730. [CrossRef]
23. Mott, R.; Brameshuber, W. Erste Erkenntnisse zum Extrudieren von Textilbeton. *TUDALIT: Leichter Bau.-Zuk. Formen* **2012**, *7*, 23.
24. Woerd, J.D. Eine Methodik zur Realisierung Dünnwandiger Faltwerke aus Zementbasierten Verbundwerkstoffen durch Faltung: Lehrstuhl und Institut für Massivbau. Ph.D. Thesis, Rheinisch-Westfälische Technische Hochschule Aachen, Aachen, Germany, 2018.
25. Du, W.; Liu, Q.; Zhou, Z.; Uddin, N. Experimental investigation of innovative composite folded thin cylindrical concrete shell structures. *Thin-Walled Struct.* **2019**, *137*, 224–230. [CrossRef]
26. Chudoba, R.; van der Woerd, J.; Schmerl, M.; Hegger, J. ORICRETE: Modeling support for design and manufacturing of folded concrete structures. *Adv. Eng. Softw.* **2014**, *72*, 119–127. [CrossRef]
27. Pidun, K.; Hannawald, J.; Koch, A. Entwicklung eines Verfahrens zur Herstellung eines Fassadenelementes aus umgeformtem Textilbeton. Forschungsprojet "ConcreteFold". *Betonw. Int. BWI* **2016**, *19*, 38–45.
28. Liew, A.; López, D.L.; van Mele, T.; Block, P. Design, fabrication and testing of a prototype, thin-vaulted, unreinforced concrete floor. *Eng. Struct.* **2017**, *137*, 323–335. [CrossRef]
29. *DIN EN 196-1:2016-11*; Methods of Testing Cement—Part 1: Determination of Strength. German Version; Beuth Verlag GmbH: Berlin, Germany, 2016. [CrossRef]
30. *DIN 53362:2003-10*; Testing of Plastics Films and Textile Fabrics (Excluding Nonwovens), Coated or Not Coated Fabrics—Determination of Stiffness in Bending—Method according to Cantilever. Beuth Verlag GmbH: Berlin, Germany, 2003. [CrossRef]
31. Woerd, J.D.; Bonfig, C.; Hegger, J.; Chudoba, R. Construction of a vault using folded segments made out of textile reinforced concrete by fold-in-fresh. In Proceedings of the IASS Annual Symposia, IASS 2017 Hamburg Symposium: Concrete Light: Innovative Concrete Constructions, Hamburg, Germany, 25–28 September 2017.